Journal of King Saud University – Science 29 (2017) 487–493

Contents lists available at ScienceDirect

Journal of King Saud University – Science

journal homepage: www.sciencedirect.com

Potential contact and intraocular lenses based on hydrophilic/hydrophobic sulfonated syndiotactic polystyrene membranes

Simona Zuppolini [a], Anna Borriello [a,*], Marina Pellegrino [b], Vincenzo Venditto [b,*], Luigi Ambrosio [a], Luigi Nicolais [c]

[a] Institute of Polymers, Composites and Biomaterials, National Research Council of Italy, Naples, Italy
[b] Department of Chemistry and Biology and INSTM Research Unit, University of Salerno, Fisciano, Salerno, Italy
[c] Materias s.r.l., University of Naples "Federico II" Campus San Giovanni a Teduccio, Naples, Italy

ARTICLE INFO

Article history:
Received 12 July 2017
Accepted 9 September 2017
Available online 11 September 2017

Keywords:
Sulfonated polystyrene
Nanoporous crystalline structure
Contact lens
Hydrophilic/hydrophobic film

ABSTRACT

Crystalline films of syndiotactic polystyrene (s-PS), a commercially available thermoplastic polymer, having a highly hydrophilic amorphous phase, were achieved by using a mild solid-state sulfonation procedure. Despite the used mild process conditions, an easy and uniform sulfonation of the phenyl rings of the amorphous phase is obtained. The crystallinity of the polymer was not affect by the sulfonation degree (*S*), at least at *S* less than 20%, and the obtained polymer films show the nanoporous crystalline form of s-PS. As widely reported in literature, the nanoporous nature of the polymer crystalline phase gives to these materials the ability to absorb and release organic molecules of appropriate size and polarity. This property, coupled to transparency, makes these materials potentially useful intraocular lens (IOLs) and contact lens applications. Sulfonation procedure and sulfonated film samples characterization by using wide-angle X-ray diffraction (WAXD), Fourier-transform infrared (FTIR) and ultraviolet-visible (UV-vis) spectroscopy techniques and water sorption tests were reported. Furthermore, the biocompatibility study demonstrated no cytotoxicity and appropriate cell interaction properties for the specific applications.

1. Introduction

In the last centenary the field of contact lens materials has been continuously evolving. The technology of vision correction uses a lens in intimate contact with the cornea which is anterior part of the eye shell (Lepore et al., 2002). The cornea is a multilayer tissue with a high water content (65–75%) whose structure is complex and mechanical properties are mainly correlated to collagen fibrils tridimensional distribution. In this context, the ocular environment places high demands on the performance of contact lenses as biomaterials. Therefore, biomaterial science has led to the development of a variety of intraocular lens (IOLs) and contact lenses biomaterials (Chehade and Elder, 1997; Kodjikian et al., 2004; Nicolson and Vogt, 2001). Main chemical-physical characteristics of these materials are optical transmittance, dimensional stability and chemical stability. Moreover, materials used in ophthalmic devices have to be non-toxic, biocompatible and anti-adhesive to avoid the lens opacification due to the adhesion, proliferation and migration of cells.

Recently, novel anti-adhesive materials have been developed to reduce the collateral effects due to cell-material interaction without affect optical properties (Lee et al., 2007). Hydrogel, soft acrylic and silicone IOLs have gradually displaced poly(methyl methacrylate) (PMMA) lenses. Silicone has the lowest threshold for YAG laser damage of all IOLs materials but, due to its hydrophobic surface, it gives a high risk of cellular reactions. Hydrogel lenses are very biocompatible and resistant to YAG laser, but pigment adheres to their surface. Soft acrylic IOLs unfold slowly, resulting in controlled insertion, but it is possible to crack the lens or develop glistenings due to water accumulation. s-PS is a commercial thermoplastic semicrystalline polymer presenting

* Corresponding authors.
E-mail addresses: borriell@unina.it (A. Borriello), vvenditto@unisa.it (V. Venditto).
Peer review under responsibility of King Saud University.

Production and hosting by Elsevier

http://dx.doi.org/10.1016/j.jksus.2017.09.004
1018-3647/

high robustness, durability, and low cost associated with easy processing. The mild conditions of the used sulfonation procedure (Borriello et al., 2009; Venditto et al., 2015), allow to selectively sulfonate only amorphous phase of s-PS leaving intact the crystalline phase. At the end of the sulfonation procedure, the polymer is in the nanoporous crystalline phase, which inside the crystal lattice presents empty spaces distributed in all identical cavities of nanometric dimensions (micropores, according to IUPAC classification). It is well known that s-PS nanoporous crystal forms, named δ (De Rosa et al., 1997) and ε (Petraccone et al., 2008), are able to absorb organic molecules of appropriate size and polarity, even if present in traces in air or water (Daniel et al., 2011, 2013a, 2013b; Guerra et al., 2012; Manfredi et al., 1997; Mensitieri et al., 2008). Moreover, the capacity of the s-PS nanoporous crystal δ form to release previously absorbed guests has been extensively studied, for gases (e.g., CO_2, ethylene, propene, and butadiene) (Albunia et al., 2012; Annunziata et al., 2006) and organic molecules (e.g., 1,2-dichloroethylene, carvacrol) (Albunia et al., 2014; Venditto et al., 2006).

In this work we summarize the preliminary characterization results on a new hydrophilic-hydrophobic membrane as potential IOLs and contact lenses material based on semicrystalline s-PS film having sulfonated amorphous phase.

2. Materials and methods

2.1. Materials

The s-PS used in this study was manufactured by Dow Chemical Company under the trademark Questra 101. The ^{13}C-NMR characterization showed that the content of syndiotactic triads was over 98%. The weight-average molar mass obtained by gel permeation chromatography (GPC) in 1,3,5-trichlorobenzene at 135 °C was found to be $M_w = 3.210^5$ with the polydispersity index $M_w/M_n = 3.9$ (Rizzo et al., 2002a).

All films considered in this paper have been obtained by casting from 0.5 wt% solutions, at room temperature from chloroform (Rizzo et al., 2002b). The films present uniplanar orientation of crystalline phases and thickness in the 30–70 μm range.

2.2. Sulfonation procedure

The sulfonation reagent was prepared by mixing an excess of lauric acid with chlorosulfonic acid ($ClSO_3H$) at room temperature, for 24 h:

$$CH_3(CH_2)_{10}COOH + ClSO_3H \rightarrow CH_3(CH_2)_{10}COOSO_3H + HCl$$

In detail, 1.6 mol of lauric acid (Aldrich, ≥98%) was used per 1.0 mol of $ClSO_3H$ (Sigma-Aldrich, 99%). The sulfonating solution was obtained by mixing 40 ml di $CHCl_3$ (Aldrich, 99%) and 4.2 g of the solution containing the acyl sulfate sulfonating reagent. The polymer sulfonation was performed by soaking s-PS films in the sulfonating solution, at temperature of 40 °C, for times from 2 to 24 h. The sulfonated films (Ss-PS) have been purified by possible residuals of the sulfonation process by washing with ethanol and $CHCl_3$, and then the solvents were extracted with carbon dioxide in supercritical conditions. The extractions were performed by using a SFX 200 supercritical carbon dioxide extractor (ISCO Inc.) using the following conditions: T = 40 °C, P = 200 bar, extraction time t = 180 min. As well established in the literature, (Ma et al., 2005; Reverchon et al., 1999) this procedure leads to δ form of s-PS.

The *S* has been evaluated by elemental analysis on the whole semicrystalline samples, by using a Flash EA 1112 analyzer from Thermo Fisher Scientific, and is reported as molar fraction of sulfonated monomeric units:

$$S = [(\text{sulfur moles by elemental analysis})/(\text{moles of polymer styrenic units})] \times 100$$

The membrane were examined with a scanning electron microscope (SEM) (Leica Cambridge Stereoscan S440) coupled with a probe for energy-dispersive scanning (EDS) to evaluate the *S* at different depths of films Ss-PS throughout the sample thickness. The membranes were cryogenically fractured in liquid N_2 and silver coated prior to EDS analysis. For the EDS calibration, the following standards were used: $CaCO_3$ (carbon standard), SiO_2 (oxygen standard), FeS_2 (sulfur standard). The EDS was performed with a beam current of 100 pA and a 20 kV acceleration voltage. As expected, only the peaks of S, C, O and Ag atoms, the latter being used as a coating element, were observed in this range of energy. The observed peaks do not have any overlaps between them. The sulfur percentage present on sample surfaces was evaluated by comparing the S and C content and using a relationship similar to that shown above.

2.3. Characterization methods

2.3.1. Wide-angle X-ray diffraction

Wide-angle X-ray diffraction (WAXD) patterns were obtained with an automatic Theta-Theta Bruker D8 Advance powder diffractometer, equipped with a Vantec PSD (multi strip position sensitive) detector, by using a nickel filtered CuKα radiation (λ = 1.5418 Å). Measurements were made in reflection, on films horizontally mounted on sample holder, in the range 2θ = 4–40°, by using 1° soller slits both on incident and diffracted beams. The correlation length of the crystalline domains, perpendicular to the (010) crystal planes was evaluated using the Scherrer formula

$$D_{hkl} = 0.9\lambda/(\beta_{hkl}\cos\theta_{hkl})$$

where β_{hkl} is the full width at half-maximum expressed in radiant units, λ is the wavelength, and θ_{hkl} the diffraction angle.

2.3.2. FT-IR spectroscopy

Infrared spectra were obtained at a resolution of 2.0 cm^{-1} by a Tensor 27 Brucker spectrometer equipped with deuterated triglycine sulphate (DTGS) detector and a Ge/KBr beam splitter. The frequency scale was internally calibrated at 0.01 cm^{-1} using a He-Ne laser. Measurements were made in transmission on dry films vertically mounted on sample holder, and 16 scans were signal averaged in order to reduce the signal-to-noise ratio. The degree of crystallinity (X_c) has been evaluated by the FT-IR spectral subtraction procedure, as described by Musto et al. (1997). In detail, the spectrum of a fully amorphous s-PS film was subtracted to the spectra of semicrystalline samples ensuring that the 1379 cm^{-1} peak, related to only the amorphous phase, was reduced close to the baseline (Albunia et al., 2006).

2.3.3. Water sorption measurements

The water content for Ss-PS with different *S* was measured as follows: the dried polymer film was immersed in distilled water at room temperature, for 24 h. The excess water on the surface of the swollen hydrogel was gently removed with a filter paper before to measure its weight, and the water content in the film was determined from an increase in the film weight. The water content responsible for the swelling of the film is expressed from following equation:

$$\textit{Water content}\ (\%) = \frac{W_{wet} - W_{dry}}{W_{wet}} \times 100$$

where W_{wet} and W_{dry} are the weights of the wet and dry samples, respectively.

The water vapor sorption of Ss-PS films was investigated by a Q5000 SA thermogravimetric analyzer from TA Instruments, containing a microbalance in which the sample and reference were enclosed in a humidity and temperature controlled chamber. The microbalance is able to operate in the temperature range of 5–85 °C, controlling the relative humidity (RH) anywhere in the 0–98% range. The temperature was controlled by Peltier elements and was therefore easily varied. Dried N_2 gas flow (200 mL min^{-1}) was split into two parts, of which one part was wetted by passing it through a water-saturated chamber. In the following, water vapor activity was expressed as p/p_0 ratio (assuming ideal gas behavior for the vapor phase and for the gas mixture, where p is the partial water vapor pressure and p_0 is the water vapor equilibrium pressure at the same temperature) and it so identified with the RH. The water vapor measurements of the samples were carried out at 30, 35, 40, 50 and 70 °C in the activity range of about 0–0.9.

2.3.4. UV-vis absorption

The optical transparency of the Ss-PS film was examined using UV-vis Agilent Technologies Cary 60 spectrophotometer. The sample was prepared by solvent evaporation method and immersed in distill water for 24 h to reach swelling equilibrium. The measurement was performed from 200 to 900 nm wavelength at room temperature.

2.4. Biological experiments

2.4.1. Cell culture

Mouse embryo fibroblast NIH3T3 were maintained at 37 °C and 5% CO_2 on Dubecco's modified Eagle medium (DMEM) supplemented with 10% fetal bovine serum (FBS, BioWhittaker) Wakersville, MD), 2 mM 1-glutamine (Sigma, St. Louis, MO), 1000 U L^{-1} penicillin (Sigma, St. Louis, MO) and 100 mg L^{-1} streptomycin (Sigma, St. Louis, MO).

2.4.2. Cell adhesion and cytotoxicity experiments

For cell adhesion experiments, $1{\cdot}10^5$ NIH3T3 cells were seeded on polystyrene plates (control) and on Ss-PS film, pre-incubated in serum free medium for 6 h, to avoid unspecific cell adhesion depending on serum protein adsorption, and then incubated in DMEM-10% FBS for the analysis. Cell distribution on polymer plates was evaluated by optical microscope observation by Optical microscope Olympus BX-51 M and the acquisition of images were made by Extended Focus Image (EFI) software.

Cell viability and proliferation were evaluated by using the Alamar Blue assay. For each plate of s-PS and Ss-PS, 2 mL of DMEM medium without Phenol Red (HyClone, UK) containing 10% v/v Alamar Blue (AbD Serotec Ltd, UK) were added, followed by incubation at 37 °C and 5% CO_2 for 4 h. The solution was subsequently removed from the plates and analyzed by a Spectrophotometer (multilabel counter, 1420 Victor, Perkin Elmer, Italy) at wavelength of 570 and 600 nm. The number of viable cells was calculated by the fluorescence values measured. Statistical analysis was carried out using one-way ANOVA at the significance level $p < 0.05$.

3. Results and discussion

3.1. Ss-PS films: structural and morphological properties

The solid state sulfonation procedure on semi-crystalline s-PS films was described for the first time by us (Borriello et al., 2009). This procedure selectively acts on the phenyl rings of the polymer amorphous phase, leaving the crystalline phase substantially unchanged. In addition, it provides a uniform distribution of the sulfonic groups throughout the film thickness, as shown in Fig. 1.

It has been hypothesized that highly permeable nanoporous crystal forms of s-PS, plasticized by the chloroform used in the sulfonation, allow rapid and uniform diffusion of sulfonating reagents inside the films and as a consequence uniform sulfonic groups distribution (Borriello et al., 2009).

In Fig. 2, the WAXD pattern of unsulfonated s-PS casting film (pattern A) is compared with those Ss-PS films having a S of 6 and 17%, pattern B and C, respectively.

In all WAXD spectra the only observed reflections are those typical of the s-PS nanoporous crystal form having uniplanar orientation (Rizzo et al., 2002a,b). In detail, peaks located at $2\theta \approx 8.4$ and 17 (d = 1.05 and 0.52 nm) correspond to the (010) and (020) reflections of the monoclinic cell unit of the s-PS nanoporous crystal form (De Rosa et al., 1997) whose a e c axes are preferentially parallel to the film plane (Rizzo et al., 2002a,b). This orientation gives the film better mechanical properties (D'Aniello et al., 2005).

WAXD spectra of sulfonated films (Fig. 2 B and C) show a progressive increase of amorphous of halo intensity when increasing S. In addition, the enlargement of the intense peak (010) with increasing S, shows a reduction in the crystal sizes, although the

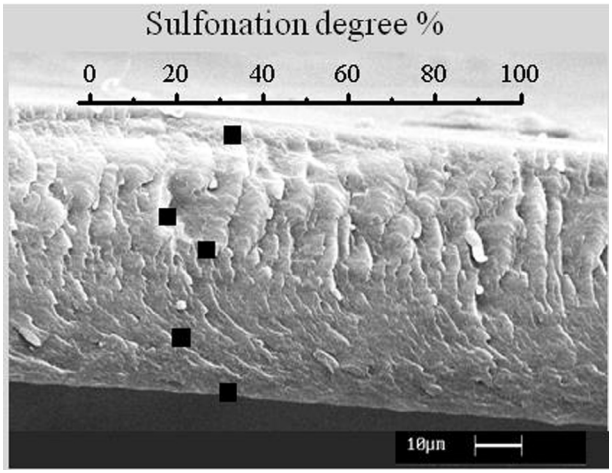

Fig. 1. SEM micrograph of a nanoporous Ss-PS film section. Black dots indicate the S valued by EDS analysis.

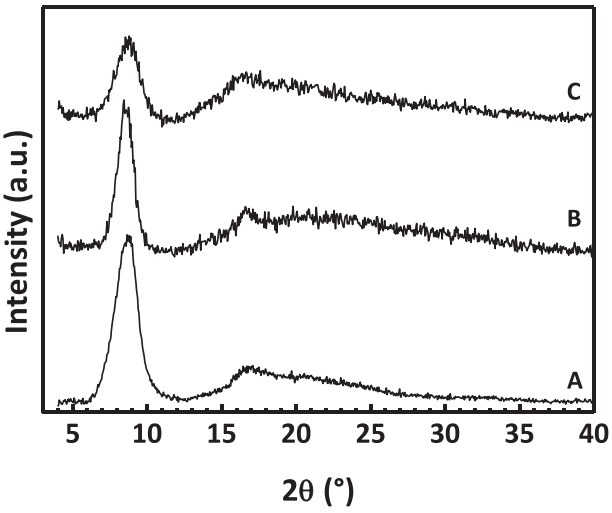

Fig. 2. WAXD patterns (CuK radiation) of Ss-PS films with $S = 0$ (A), $S = 6\%$ (B) and $S = 17\%$ (C).

nature of the crystalline phase is essentially unaltered. In detail, the full width at half maximum of the (0 1 0) peak is 1.2 and 1.9° for pattern A ($S = 0\%$) and C ($S = 17\%$), respectively, which correspond to a reduction from 6.6 to 4.3 nm of correlation length of the crystalline domains.

FT-IR spectra of unsulfonated s-PS casting film (curve A) and those of Ss-PS films having a S of 6 and 17%, curve B and C respectively, are compared in Fig. 3. All the FT-IR spectra present the typical infrared absorbance bands of the s-PS nanoporous crystal phase (which are located at 1354, 1320 e 1277 cm^{-1}) (Musto et al., 1997). The peak at 1412 cm^{-1}, only present in the spectra B and C, is due to sulfonation and it increases with the increasing of S. A crystallinity degree ranging from ≈35 to 50%, evaluated by using a procedure described by Albunia et al. (2006) was observed. It is worth noting that, with increasing S, the infrared bands of s-PS nanoporous crystal phase are only slightly reduced, so that crystallinity of Ss-PS film with S of 17% is comparable with that of unsulfonated film.

3.2. Characterization of partially sulfonated s-PS as material for contact lens

Described results suggested to evaluate the Ss-PS as potential material for IOLs and contact lenses. Hence, some of the key features required for this application have been evaluated such as water sorption, optical transparency and cytotoxicity on this hydrophilic/hydrophobic membrane.

3.2.1. Water sorption

The capacity of the contact lens material to absorb water and swell is very important. It is a property that mainly depends on the ratio of hydrophilic/hydrophobic functional groups of the polymer and on the nature of these groups as well (Muter, 2015). As hydrogels consist of cross-linked networks, they generally have an ability to absorb considerable amounts of water. Sulfonation of the amorphous phase gives s-PS films hydrophilic properties maintaining unaltered hydrophobic feature and the sorption capacity of the nanoporous crystalline phase. In Fig. 4, the water uptake in Ss-PS films with different S, is shown. Swelling data, calculated by measuring the size change of a rectangular film (10 × 20 mm, 100 μm thick), range from 0 to 40%, for membranes with S ranging from 0 to 30%, respectively. In detail, the Ss-PS film with $S = 17\%$ showed a swelling of 32%.

It is worth noting that, after the water removal the nanoporous nature of the crystalline phase is maintained without a significant reduction in crystallinity. As an example, in the Ss-PS film with $S = 17\%$, crystallinity, estimated by using FT-IR analysis on dry samples, remains close to 30%. Swelling data calculated by measuring the size change of a rectangular film (10 × 20 mm, 100 μm thick) emerged as 40%. The sulfonation of s-PS film in its clathrate form introduces sulfonic acid groups on the side phenyl groups of the polymer backbone to obtain a hydrophilic membrane with hydrophobic crystalline nanoporosity able to guest molecules. In fact, as confirmed by FT-Raman Spectroscopy (Musto et al., 2010), the amorphous regions supply hydrophilic sulfonated regions while the clathrate crystalline regions, which result unaffected by the reaction, represent the hydrophobic phase. This allows to obtain high S samples (≥50 mol%), water-insoluble, which swell extensively in water. For example, this could enables implantation of a semi-hydrated lens through a small incision, also with the advantage of small drug molecules delivery.

On the basis of described results, $S = 17\%$ was identified as the most suitable S of s-PS to be studied as potential material as IOLs and contact lens. Hence, the following experiments were performed on 17% Ss-PS.

Water vapor sorption was evaluated for 17% Ss-PS at different temperatures by thermogravimetric measurements and it is reported in Fig. 5A as function of water vapor activity. Results indicated that the sorption is not significantly quite dependent on temperature in the 20–60 °C range, and it is higher than common soft lens hydrogel materials such as Polymacon (Weinmüller et al., 2006), especially at higher water activity (Fig. 5B).

3.2.2. Optical transparency

For a material to be suitable for contact lenses it must have transmittance properties not only for ultraviolet radiation (UVR) protective properties (Moore and Ferreira, 2006), but also for visual performance (Muter, 2015).

As showed in UV-vis spectrum (Fig. 6), an ultraviolet radiation wavelength cutoff is only evident below 300 nm while in the visible light wave range of 400–700 nm no absorbance is practically measured. Hence, optical transparency, which is correlated to absorbance (A = −logT), results relatively constant and approximatively ≥95%, that is comparable to data of common contact lens material (Faubl and Quinn, 2000), as well as a high UV protection .

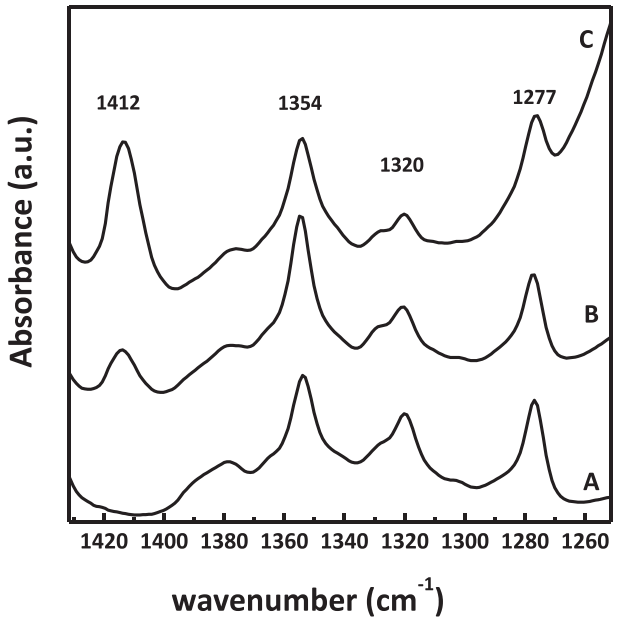

Fig. 3. FT-IR of s-PS films with $S = 0$ (A), $S = 6\%$ (B) and $S = 17\%$ (C). The peaks associated with the s-PS nanoporous crystal phase (1354, 1320, and 1277 cm^{-1}) and the peak associated with S (1412 cm^{-1}) is indicated.

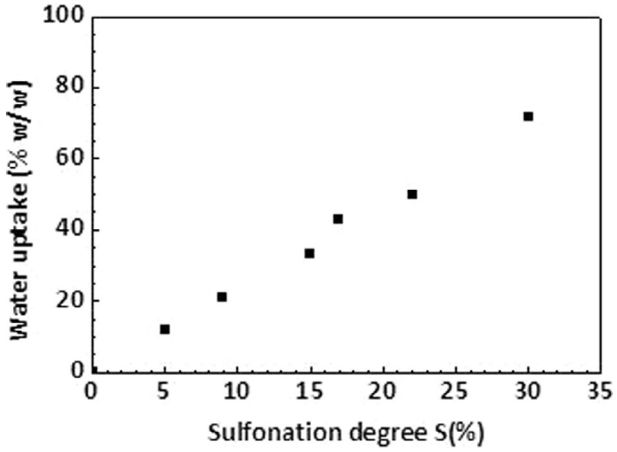

Fig. 4. Liquid water uptake of nanoporous Ss-PS films vs S.

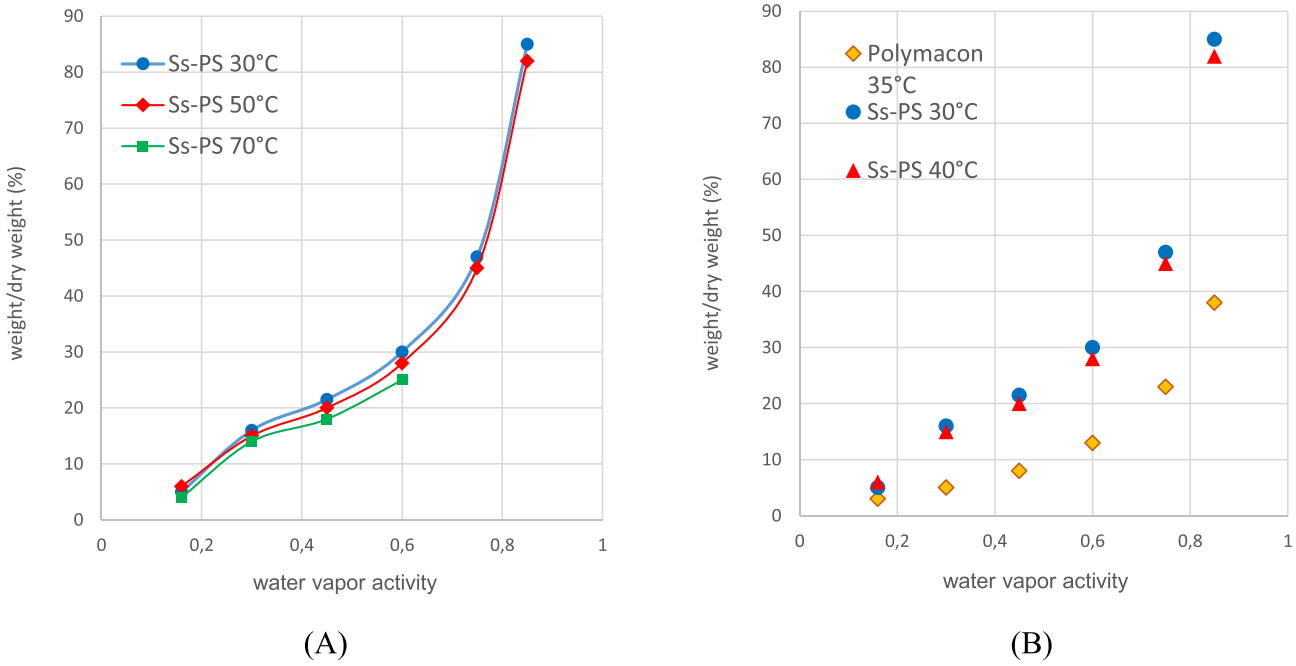

Fig. 5. Water vapor uptake of Ss-PS at different temperatures (A) and compared with Polymacon (B).

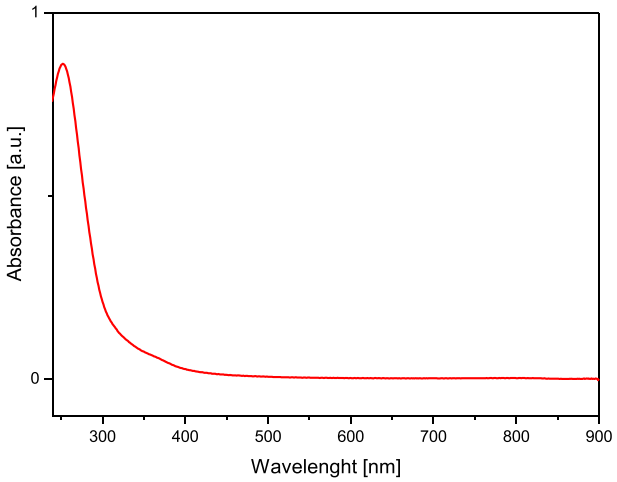

Fig. 6. UV-vis absorption spectrum of 17% Ss-PS film.

3.3. Biological experiments

In order to evaluate cytotoxicity of a material many indirect known methodologies exist which measure cell proliferation and viability (Ahmed et al., 1994; Mosmann, 1983; Squatrito et al., 1995). Among all, the one-step Alamar Blue (AB) assay is probably the most used for quantifying *in vitro* viability of various cells (Ahmed et al., 1994; Fields and Lancaster, 1993) due to its numerous advantages (Nakayama et al., 1997). The water-soluble Alamar Blue dye is an alternative fluorogenic indicator of the cellular redox state, which in cell proliferation is reduced from a blue non-fluorescent form to a red fluorescent product due to metabolic activity of the cultured cells (Gloeckner et al., 2001). The redox reaction of Alamar Blue dye that occurs into growing cells culture is a reflection of cell viability, can be quantified by its optical density or fluorescence for greater sensitivity. On this basis, by measuring the fluorescence value of the sample it is possible to trace the number of cells. Cytotoxicity of the Ss-PS films was indirectly evaluated by using Alamar Blue assay and viable cells count was calculated against untreated controls. The results (Fig. 7) are analyzed from five experiments on polymer samples, and there was a statistically significance of $p < 0.05$ in the cell number over the culture period. NIH3T3 cells appeared to be not sensitive to the growth inhibitory effects of Alamar Blue, therefore the material results non-cytotoxic.

Cell adhesion on the polymer films was evaluated by optical microscope observation (Fig. 8). In particular, NIH3T3 cells appear fusiform and aligned on polystyrene films (A) while round and isolated on the Ss-PS films (B), thus indicating a low adhesion to the material also confirmed by the count of adhered cell number which is lower than on control surfaces (Fig. 8C).

This result enhanced anti-adhesive properties useful to avoid cell adhesion, proliferation and migration which cause opacification phenomena on lenses, particularly injurious in IOLs uses. Indeed, it is well known capsular opacification mainly occurs on the posterior side, usually referred to as posterior capsular opacification, that occurs in approximately half the cases 2–5 years after the surgery (Bozukova et al., 2007).

Among the many suitable properties, a good elasticity of materials is generally required to provide contact lenses which are easier to fit and more comfortable to wear (Nicolson and Vogt, 2001). In addition, has developed preferring foldable IOLs and

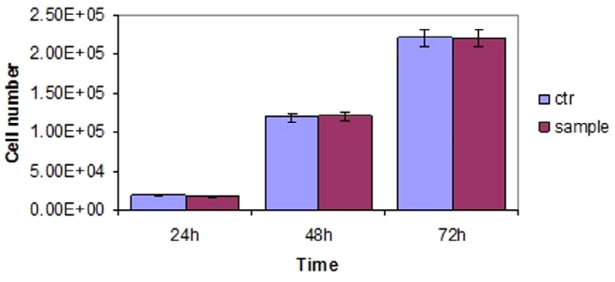

Fig. 7. Indirect cytotoxicity assay (Alamar Blue): evaluation of proliferation cell rate on control surface (polystyrene) and Ss-PS film (sample) with a statistical significance of $p < 0.05$.

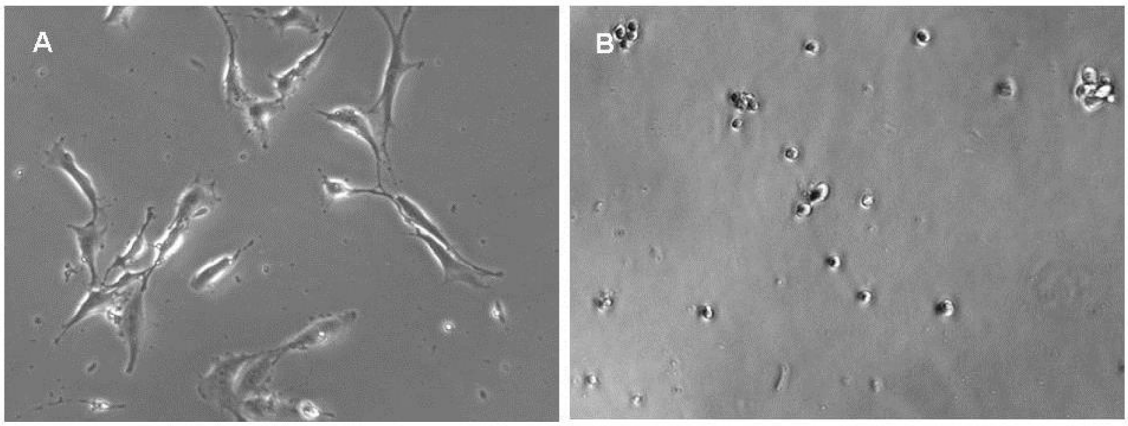

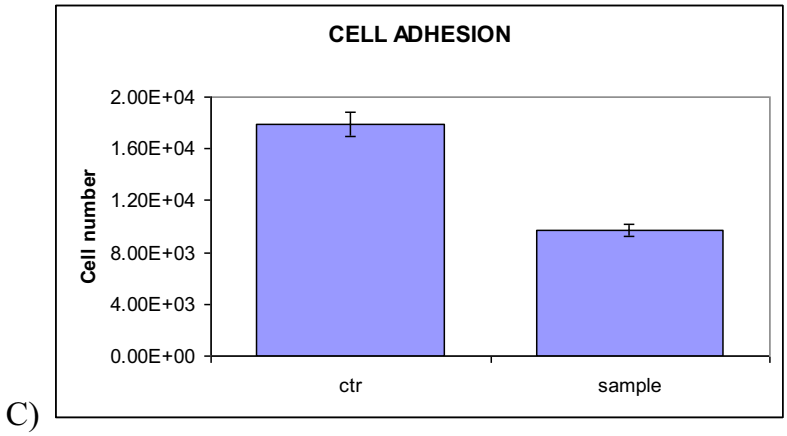

C)

Fig. 8. Optical micrographs of NIH3T3 cells seeded on polystyrene plate (A) and on Ss-PS film (B). (C) Cell adhesion results for control surface (polystyrene) and Ss-PS film (sample) with a statistical significance of $p < 0.05$.

especially those suitable for micro incision cataract surgery (MICS), i.e. those IOLs that can be implanted through sub-2 mm incision (Antoniac et al., 2015). From a preliminary observation these materials would own a good elasticity, when a like lens 17% Ss-PS film was manually folded by using a tweezer (Fig. 9). This property minimize YAG laser damaging while their hydrophilic nature reduces mechanical friction with ocular tissues.

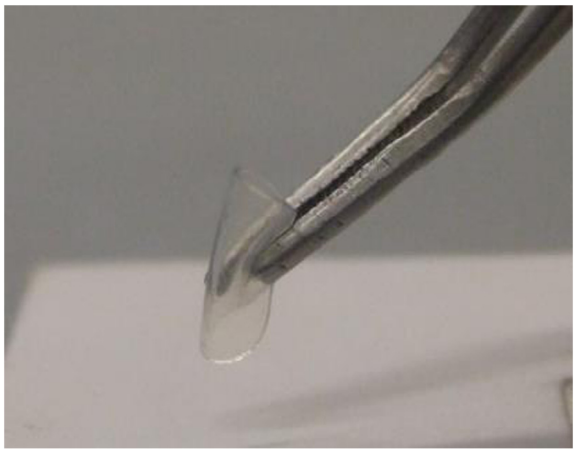

Fig. 9. Picture of manually folded Ss-PS lens.

4. Conclusions

The results obtained confirm that it is possible to control chemical and physical characteristics of the final polymeric product, such as hydrophilicity, hydrophobicity, water content, optical clarity, adhesive properties, permeability and other mechanical properties.

Preliminary characterization results on partially sulfonated (17%) s-PS membranes show a good elasticity and optical transparency, a high water-vapor sorption and a low cell adhesion, confirming that this new hydrophilic-hydrophobic material is a potential candidate for IOLs and contact lenses application. Further experiments and tests are in progress to verify the feasibility in this application.

References

Ahmed, S.A., Gogal, R.M.J., Walsh, J.E., 1994. A new rapid and simple non-radioactive assay to monitor and determine the proliferation of lymphocytes: an alternative to [3H]thymidine incorporation assay. J. Immunol. Methods 170, 211–224.

Albunia, A.R., Musto, P., Guerra, G., 2006. FT-IR spectra of pure helical crystalline phases of syndiotactic polystyrene. Polymer 47, 234–242.

Albunia, A.R., Venditto, V., Guerra, G., 2012. Infrared linear dichroism as a tool to evaluate volatile guest partition between amorphous and nanoporous-crystalline polymer phases. Polym. Sci. Part B: Polym. Phys. 50, 1474–1479.

Albunia, A.R., Rizzo, P., Ianniello, G., Rufolo, C., Guerra, G., 2014. Syndiotactic polystyrene films with a co-crystalline phase including carvacrol guest molecules. J. Polym. Sci., Part B Polym. Phys. 52, 657–665.

Annunziata, L., Albunia, A.R., Venditto, V., Mensitieri, G., Guerra, G., 2006. Polymer/gas clathrates for gas storage and controlled release. Macromolecules 39, 9166–9170.

Antoniac, I.V., Burcea, M., Ionescu, R.D., Balta, F., 2015. IOL's opacification: a complex analysis based on the clinical aspects, biomaterials used and surface characterization of explanted IOL's. Mater. Plast. 52, 109–112.

Borriello, A., Agoretti, P., Ambrosio, L., Fasano, G., Pellegrino, M., Venditto, V., Guerra, G., 2009. Syndiotactic polystyrene films with sulfonated amorphous phase and nanoporous crystalline phase. Chem. Mater. 21, 3191–3196.

Bozukova, D., Pagnoulle, C., De Pauw-Gillet, M.-C., Desbief, S., Lazzaroni, R., Ruth, N., Jérôme, R., Jérôme, C., 2007. Improved performances of intraocular lenses by poly(ethylene glycol) chemical coatings. Biomacromolecules 8, 2379–2387.

Chehade, M., Elder, M.J., 1997. Intraocular lens materials and styles: a review. Aust. Nz. J. Ophthalmol. 25, 255–263.

D'Aniello, C., Rizzo, P., Guerra, G., 2005. Polymorphism and mechanical properties of syndiotactic polystyrene films. Polymer 46, 11435–11441.

Daniel, C., Longo, S., Vitillo, J.G., Fasano, G., Guerra, G., 2011. Nanoporous crystalline phases of poly(2,6-dimethyl-1,4-phenylene)oxide. Chem. Mater. 23, 3195–3200.

Daniel, C., Zhovner, D., Guerra, G., 2013a. Thermal stability of nanoporous crystalline and amorphous phases of poly (2, 6-dimethyl-1, 4-phenylene) oxide. Macromolecules 46, 449–454.

Daniel, C., Longo, S., Ricciardi, R., Reverchon, E., Guerra, G., 2013b. Monolithic nanoporous crystalline aerogels. Macromol. Rapid Commun. 34, 1194–1207.

De Rosa, C., Guerra, G., Petraccone, V., Pirozzi, B., 1997. Crystal structure of the emptied clathrate form (δe form) of syndiotactic polystyrene. Macromolecules 30, 4147–4152.

Faubl, H., Quinn, M.H., 2000. Spectra of UV-absorbing contact lenses: relative performance. Int. Cont. Lens Clin. 27, 65–74.

Fields, R.D., Lancaster, M.V., 1993. Dual-attribute continuous monitoring of cell proliferation/cytotoxicity. Am. Biotechnol. Lab. 11, 48–50.

Gloeckner, H., Jonuleit, T., Lemke, H.-D., 2001. Monitoring of cell viability and cell growth in a hollow-fiber bioreactor by use of the dye Alamar Blue. J. Immunol. Methods 252, 131–138.

Guerra, G., Daniel, C., Rizzo, P., Tarallo, O., 2012. Advanced materials based on polymer co-crystalline forms. J. Polym. Sci., Part B Polym. Phys. 50, 305–322.

Kodjikian, L., Burillon, C., Roques, C., Pellon, G., Renaud, F., Hartmann, D., Freney, J., 2004. Intraocular lenses, bacterial adhesion and endophthalmitis prevention: a review. Biomed. Mater. Eng. 14, 395–409.

Lee, H.I., Kim, M.K., Ko, J.H., Lee, H.J., Wee, W.R., Lee, J.H., 2007. The efficacy of an acrylic intraocular lens surface modified with polyethylene glycol in posterior capsular opacification. J. Korean Med. Sci. 22, 502–507.

Lepore, D., Ambrosio, L., De Santis, R., Nicolais, L., Scullica, L., 2002. The Eye. In: Barbucci, R. (Ed.), Integrated Biomaterials Science. Kluver Academic/Plenum Publishing Co, New York, pp. 367–379.

Ma, W., Yu, J., He, J., 2005. Empty δ crystal as an intermediate form for the δ to γ transition of syndiotactic polystyrene in supercritical carbon dioxide. Macromolecules 38, 4755–4760.

Manfredi, C., Del Nobile, M.A., Mensitieri, G., Guerra, G., Rapacciuolo, M., 1997. Vapor sorption in emptied clathrate samples of syndiotactic polystyrene. J. Polym. Sci., Part B Polym. Phys. 35, 133–140.

Mensitieri, G., Larobina, D., Guerra, G., Venditto, V., Fermeglia, M., Pricl, S., 2008. Chloroform sorption in nanoporous crystalline and amorphous phases of syndiotactic polystyrene. J. Polym. Sci., Part B Polym. Phys. 46, 8–15.

Moore, L., Ferreira, J.T., 2006. Ultraviolet (UV) transmittance characteristics of daily disposable silicone hydrogel contact lenses. Cont. Lens Anterior Eye 29, 115–122.

Mosmann, T., 1983. Rapid colorimetric assay for cellular growth and survival: application to proliferation and cytotoxicity assays. J. Immunol. Methods 65, 55–63.

Musto, P., Tavone, S., Guerra, G., De Rosa, C., 1997. Evaluation by Fourier transform infrared spectroscopy of the different crystalline forms in syndiotactic polystyrene samples. J. Polym. Sci., Part B Polym. Phys. 35, 1055–1066.

Musto, P., Borriello, A., Agoretti, P., Napolitano, T., Di Florio, G., Mensitieri, G., 2010. Selective surface modification of syndiotactic polystyrene films: a study by Fourier transform-and confocal-Raman spectroscopy. Europ. Polym. J. 46, 1004–1015.

Muter, M.A., 2015. Synthesis and biocompatibility of new contact lenses based on derivatives of 2-hydroxyethyl methacrylate and 2-ethylhexyl methacrylate. Int. J. Res. Stud. Biosci. 3, 1–9.

Nakayama, G.R., Caton, M.C., Nova, M.P., Parandoosh, Z., 1997. Assessment of the Alamar Blue assay for cellular growth and viability in vitro. J. Immunol. Methods 204, 205–208.

Nicolson, P.C., Vogt, J., 2001. Soft contact lens polymers: an evolution. Biomaterials 22, 3273–3283.

Petraccone, V., Ruiz de Ballesteros, O., Tarallo, O., Rizzo, P., Guerra, G., 2008. Nanoporous polymer crystals with cavities and channels. Chem. Mater. 20, 3663–3668.

Reverchon, E., Guerra, G., Venditto, V., 1999. Regeneration of nanoporous crystalline syndiotactic polystyrene by supercritical CO_2. J. Appl. Polym. Sci. 74, 2077–2082.

Rizzo, P., Albunia, A.R., Milano, G., Venditto, V., Guerra, G., 2002a. Crystalline orientation and molecular transport properties in nano-porous syndiotactic polystyrene films. Macromol. Symp. 185, 65–75.

Rizzo, P., Lamberti, M., Albunia, A., Ruiz de Ballesteros, O., Guerra, G., 2002b. Crystalline orientation in syndiotactic polystyrene cast films. Macromolecules 35, 5854–5860.

Squatrito, R.C., Connor, J.P., Buller, R.E., 1995. Comparison of a novel redox dye cell growth assay to the ATP bioluminescence assay. Gynecol. Oncol. 58, 101–105.

Venditto, V., De Girolamo Del Mauro, A., Mensitieri, G., Musto, P., Rizzo, P., Guerra, G., 2006. Anisotropic guest diffusion in the δ crystalline host phase of syndiotactic polystyrene: transport kinetics in films with three different uniplanar orientations of the host phase. Chem. Mater. 18, 2205–2210.

Venditto, V., Pellegrino, M., Califano, R., Guerra, G., Daniel, C., Ambrosio, L., Borriello, A., 2015. Monolithic polymeric aerogels with VOCs sorbent nanoporous crystalline and water sorbent amorphous phases. ACS Appl. Mater. Interfaces 7, 1318–1326.

Weinmüller, C., Langel, C., Fornasiero, F., Radke, C.J., Prausnitz, J.M., 2006. Sorption kinetics and equilibrium uptake for water vapor in soft-contact-lens hydrogels. J. Biomed. Mater. Res. Part A 77, 230–241.